

Supplementary Material

1 Supplementary Material and Methods

1.1 Animals

Thirty-three mice of three genetically modified mouse models were obtained from different laboratories (Laboratory of Physiopharmacology, University of Antwerp; Experimental Vascular Surgery, LUMC; CARIM MUMC) to study the presence of atherosclerosis. Four ApoE^{-/-} on a chow diet at the age of 50-52w (M and F), eight ApoE^{-/-} on Western-type diet (WD) at the age of 28-41 weeks (M and F), twelve ApoE^{-/-}Fbn1^{C1039G+/-} on WD at the age of 21-41 weeks (F) and eight ApoB100/LDLr^{-/-} mice (M and F) ranging from 37-41 weeks of age (also shown in table 1). ApoE^{-/-} and ApoE^{-/-}Fbn1^{C1039G+/-} were fed a WD from 6 weeks of age until sacrifice, hApoB100/LDLr^{-/-} female mice from 12 weeks of age until sacrifice and ApoB100/LDLr^{-/-} male mice from 32 weeks of age until sacrifice. Food and water were available ad libitum. For all ApoE^{-/-} and ApoE^{-/-}Fbn1^{C1039G+/-} mice the complete head and neck including the vascular tree were retrospectively harvested from other experimental studies and complemented with ApoB100/LDLr^{-/-} mice, leading to differences between the experimental groups in age and diet (23). Differences in ages additionally occurred due to premature death (table 1). In addition, seven 10-week-old ApoE^{-/-} and six 16-week-old C57Bl/6 chow-fed mice were used for immunohistochemical analyses. All studies were approved by local ethical committees and were performed in accordance with national and European regulations.

1.2 MRI

A magnetic resonance angiogram was made as an anatomical reference. A C57Bl/6J mouse was anaesthetized with isoflurane 1-2% and imaged using a horizontal 7T magnet (Pharmascan, Bruker, Rheinstetten, Germany) with a circular polarized MRI transceiver coil for 1H with an inner diameter of 23 mm. Bruker Paravision 5.1 software was used for image acquisition. A T2 3D Flash sequence was used to image linear flow in the mouse neck and head with the following parameters: TR 15ms, TE 2.6ms, NA 4, matrix 256*256*256, FOV 17*17*20mm, FA 30°, resolution 66x66x78 µm/pixel, scan time 36 min. The vasculature segmentation was done with AMIRA (version 9.0).

1.3 CT

A CT scan was made for a three-dimensional overview of the vascular tree and its entry into the skull. A mouse head was perfused with MicroFil (Flow Tech, Carver, MA, USA). A CT scanner (Skyscan 1076, Bruker, Rheinstetten, Germany) connected to a camera (Princeton Instruments, Trenton, USA) was used to image the vasculature with the following parameters: Alu 0.5mm filter, exposure time 1750ms, voltage 48kV, current 200µA. Reconstruction was done with NRecon (version 1.5.1.4), resulting in an image 1780x1760 pixels. Empty edges of the pictures were cropped with Photoshop (Adobe Photoshop CS6). Vasculature and bone segmentation was done with AMIRA (version 9.0).

1.4 Histology and immunohistochemistry

Mice were sacrificed by transcardial perfusion with PBS and 4% PFA after Pentobarbital injection (150 mg/kg IP) or by CO₂ inhalation. The heads were post-fixed in 4% PFA and placed for 3-4 weeks in 12.5% EDTA for decalcification. The skin was dissected from the skull and the heads were embedded in paraffin. Sections of atherogenic mice were cut at 10µm thickness and every fifth section was stained with haematoxylin and eosin (HE) to assess the distribution of atherosclerotic lesions, ranging from foam cell detection in the vessel wall to advanced atherosclerotic plaques as defined by the AHA classification (24, 25). Lesions at the common carotid artery (CCA) bifurcation were classified according to the AHA classification.

The skulls of seven non-perfused 10 weeks old ApoE^{-/-} mice and six 16 weeks old C57Bl/6 mice were decalcified and cut transversely at 5µm thickness for a more detailed immunofluorescence (ApoE^{-/-}) or immunohistochemical (C57Bl/6) analysis of vessel characteristics and morphology. HE stainings were used to determine seven areas of interest (see figure 1B): just below the CCA bifurcation (nr. 1), internal carotid artery (ICA) before the bifurcation with the pterygopalatine artery (Ptgpal) (nr. 2), ICA after the bifurcation with the Ptgpal (nr. 3), ICA just below the skull base (nr. 4), ICA within the skull base (nr. 5), ICA just above the skull base (nr. 6), ICA at the start of circle of Willis (CoW) before the bifurcations to the posterior cerebral artery (PCA) and middle cerebral artery (MCA) (nr. 7). Adjacent sections were used for Elastica van Gieson (EvG) staining and immunofluorescence or immunohistochemistry using antibodies listed in supplemental table 1 and 2.

Human formalin fixed paraffin embedded (FFPE) samples of the CCA's and basilar artery (BA), obtained from 16 autopsy patients were used to perform immunofluorescence and confocal microscopy. The patient population (n=16) had a mean age of 67 years (range 32 – 92 years), and had a fairly even gender distribution (males: females=9:7). Causes of death were neurological (n=7), unknown (n=6), cardiovascular (n=2) and infectious disease (n=1). Patient characteristics can be found in supplemental table 3. All samples were obtained after written informed consent from the donors' next of kin.

Tissue sections were cut, mounted and dewaxed in xylene and rehydrated in graded steps of ethanol. Heat-induced epitope retrieval was performed in a pretreatment module (Thermo Fisher Scientific, Fremont, CA) using Tris-EDTA for 20 minutes at 98°C. Prior to staining with the primary antibody, a protein block (Superblock, Immunologic, Duiven The Netherlands) was applied. For all washing steps a Tris-buffered saline solution was used. Double stains were performed by combining CD31, an endothelial cell marker, with one of the following oxidative stress markers HO-1, eNOS and NRF2. The dilutions used are shown in supplemental table 4, all antibodies were diluted in antibody diluent (Immunologic). All slides were coverslipped with prolong gold with DAPI (Thermo Fisher).

1.5 Image analysis

Image acquisition of the immunofluorescence stained ApoE^{-/-} mouse skulls and human FFPE samples was performed on a Leica TCS SP8 X confocal microscope (Leica Microsystems, Wetzlar, Germany). Pictures of the endothelial cells were taken at 40x magnification. Image pro premier

(media cybernetics version 9.2) was used for digital analysis of the pictures. The outline of the positive area in the CD31 stained pictures were used to determine the region of interest. Within this region the fluorescence intensity for the oxidative stress markers was assessed.

Bright-field image acquisition of the HE, EvG and immunohistochemistry stainings were taken using a Leica DM5000B microscope equipped with a DFC500 camera at 20x magnification (Leica Microsystems, Wetzlar, Germany) and LAS v4.5 software. Image analysis was performed with Image Pro Premier 9 (Media Cybernetics, Rockville, USA) to determine the optical density (OD) for PermaBlue stained IHC and the percent positive area. The vessel wall intima and media were selected as regions of interest for all stainings and vessels. Regions of interest of right and left arteries were averaged. Vessel wall thickness was measured on the HE stained sections.

1.6 Cell culture and treatments

The immortalized human brain endothelial cell line hCMEC/D3 was cultured as described previously (26, 27) and used at passages 27-33. Cells were treated with human oxLDL (BT-910, Biomedical technologies inc.) with TBARS ranging from 26.6 to 41.9nmol of MDA/mg protein (Alfa Aesar, Ward Hill, MA, USA). Uptake of the oxLDL was confirmed with Dil-oxLDL (BT-920, Alfa Aesar, Ward Hill, MA, USA) and FACS analysis, quenching for surface fluorescence with Trypan blue.

1.7 RNA isolation and real-time quantitative PCR

hCMEC/D3 cells were stimulated for 6h and 24h with 50 μ g/ml and 100 μ g/ml oxLDL (n=4), harvested using TRIzol reagent (Invitrogen, Carlsbad, CA, USA) followed by the RNA isolation procedure following manufacturer's guidelines. cDNA synthesis was performed with 1 μ g RNA using the high capacity cDNA reverse transcription kit following manufacturer's guidelines (Applied Biosystems, Foster City, CA, USA). cDNA was amplified using SYBR Green PCR Master Mix (Applied Biosystems) in a final volume of 10 μ l on a ViiaTM 7 Real-Time PCR System (Applied Biosystems) using the following HO-1 primers: HO-1 forward 5'-TGGAGCGTCCGCAAC-3' and reverse 5'-TCCTTCAGGGTCTCTGACAA-3'. Expression levels were normalized to beta-2-microglobulin (forward 5'-GTATGCCTGCCGTGTGAAC-3' and reverse 5'-AAAGCAAGCAAGCAGAATTTGG-3') and the 2- $\Delta\Delta$ CT method was used for data analysis (28).

1.8 Western blotting and nuclear fractioning

To determine HO-1 protein levels using western blotting, hCMEC/D3 cells were cultured in 6 well microplates and stimulated for 24h with oxLDL (n=3). Cells were lysed in cell lysis buffer (Cell Signaling Technology Inc, Boston, MA, USA) containing complete protease inhibitor cocktail (Roche, Almere, The Netherlands). Lysates were taken up in SDS sample buffer (100mM Tris-HCL pH 6.8, 4% SDS, 20% glycerol, 5% β -mercaptoethanol) and heated to 95 $^{\circ}$ C for 5min. Lysates were resolved on a 10% SDS-polyacrylamide gel electrophoresis, blotted to PVDF membranes (Bio-Rad Laboratories, Berkeley, CA, USA) and incubated over night at 4 $^{\circ}$ C with the primary antibodies rabbit- α -HO-1 (1:1000, Enzo Life Sciences, Farmingdale, NY, USA) and goat- α -actin (for normalization, 1:400; Santa Cruz Biotechnology) in Odyssey blocking buffer (LI-COR, Lincoln, AK,

USA) diluted 1:1 in PBS and after blocking with Odyssey blocking buffer for 1h at RT. Respective IRDye infrared fluorescent dyes secondary antibodies and the Odyssey infrared imaging system (LICOR) were used for visualization and quantification of protein levels.

To determine NRF2 nuclear protein levels, hCMEC/D3 cells were cultured in 6 well microplates (2 wells per condition) and stimulated for 4h with oxLDL (n=3). Cells were washed with ice-cold PBS and lysed and fractioned using the NE-PER nuclear and cytoplasmic extraction kit following the manufacturer's instructions (Thermo Scientific, Rockford, IL, USA). Western blotting was performed as described above and using the primary antibodies rabbit- α -Nrf2 (1:400, Santa Cruz Biotechnology, Dallas, TX, USA), goat- α -lamin B (1:200, to normalize nuclear fraction; Santa Cruz Biotechnology, Dallas, TX, USA) and goat- α -actin (1:400, to normalize cytoplasmic fraction; Santa Cruz Biotechnology, Dallas, TX, USA). Quantification of protein bands was performed using Odyssey imaging software. Fluorescence intensity was measured in an area surrounding the protein bands, and subtracted by the same area without bands for lane background correction. Relative NRF2 protein levels were obtained by correcting for loading control (actin or lamin B) levels in each sample.

1.9 ROS measurement using flow cytometric analysis

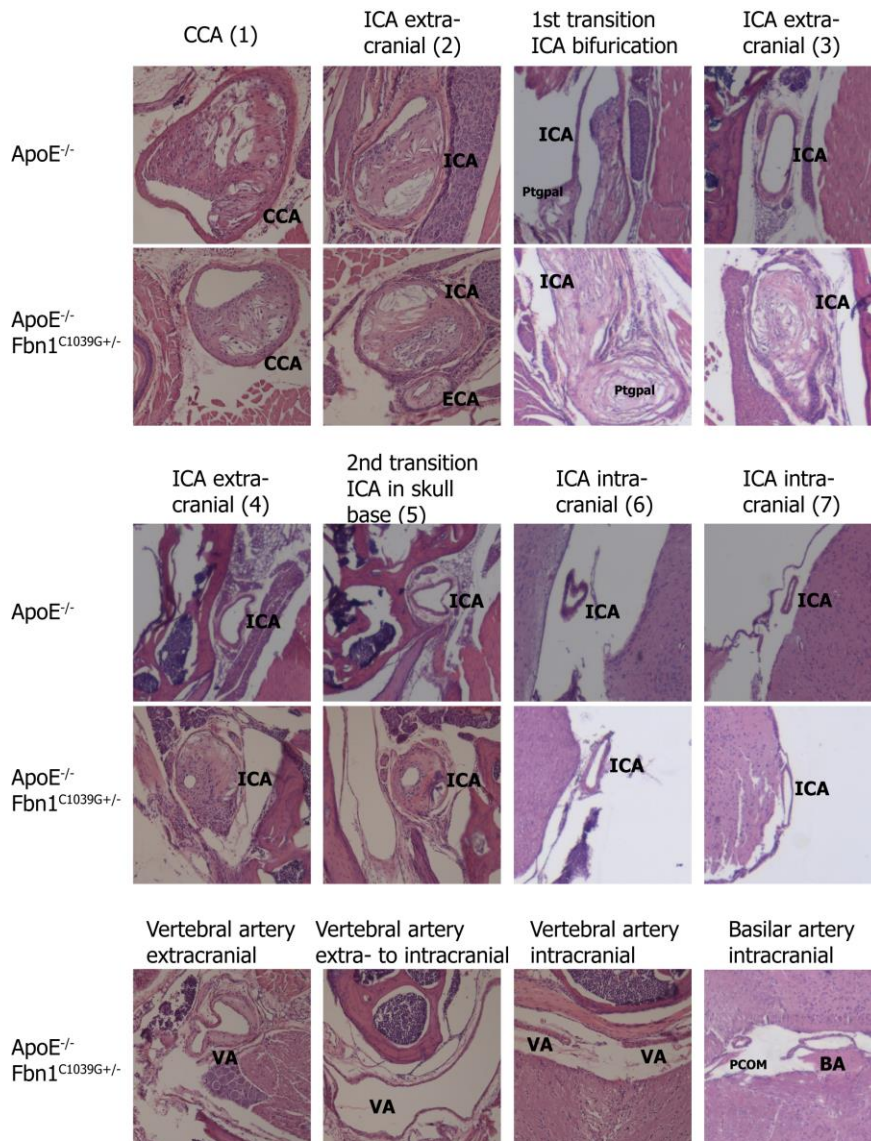
hCMEC/D3 were cultured in 24 well plates and stimulated with 50 μ g/ml and 100 μ g/ml oxLDL for 24h. Cells were washed and incubated at 37°C for 1h with the intracellular ROS detection probe CM-H2DCFDA (Invitrogen, Carlsbad, CA, USA). Endogenous ROS production was measured by measuring the median fluorescence intensity of 10.000 viable cells using a FACSCalibur flow cytometer (Becton & Dickinson, San Jose, CA, USA). The effects of oxLDL on endothelial ROS production was analyzed in both unstimulated and immune-activated cells, treated with a combination of TNF α / IFN γ (5ng/ml each, 24h).

1.10 Statistical analysis

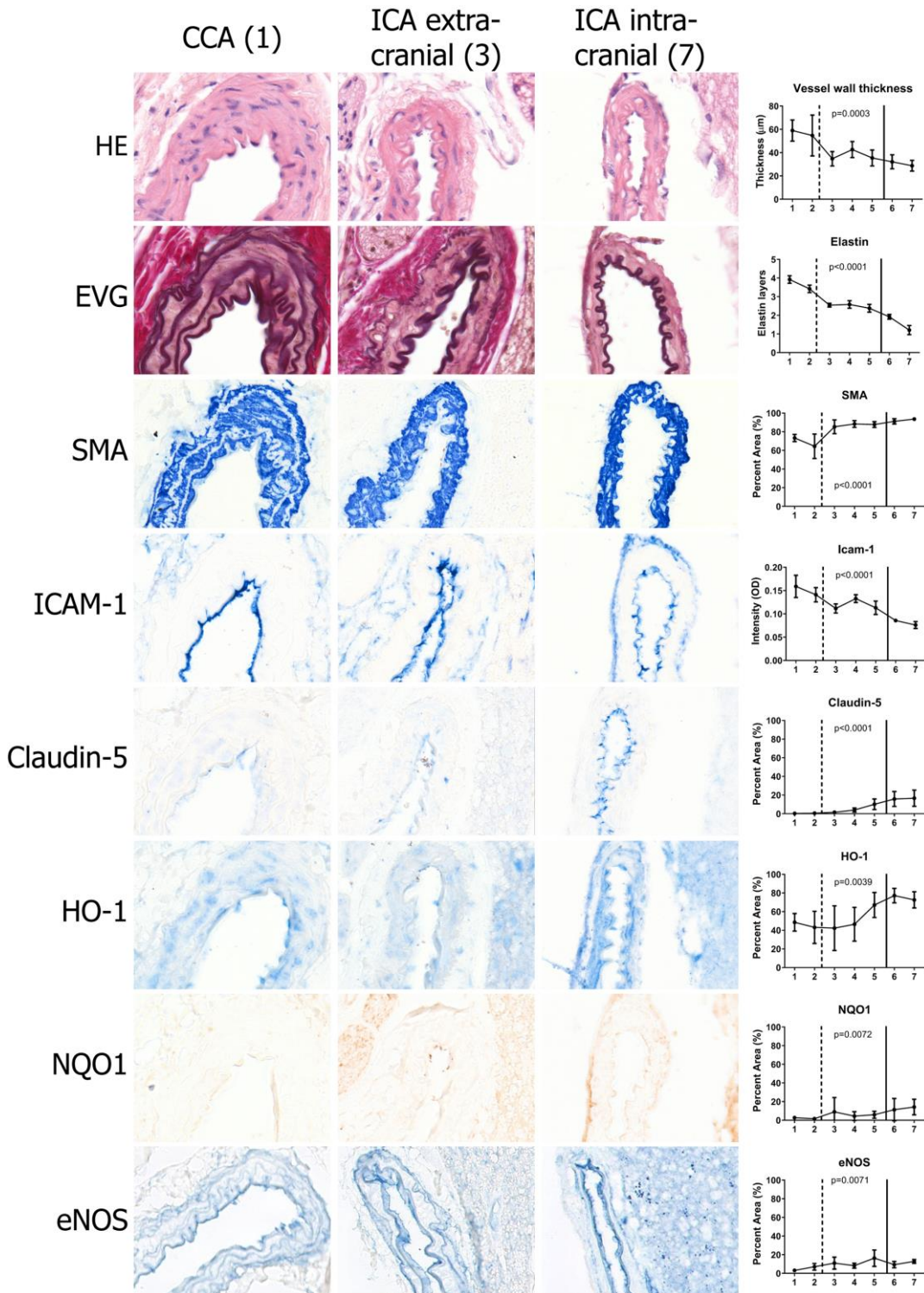
Data was analyzed using Graphpad Prism software (v5.01, La Jolla, CA, USA). Mouse immunohistochemical measures were considered statistically significant if $p < 0.05$ by Friedman test. Posthoc tests were done with Dunns test to compare all pairs of columns. Human immunohistochemical measures were considered statistically significant if $p < 0.05$ determined by a Wilcoxon signed ranked test. *In vitro* results are shown as median \pm standard deviation for FACS results and as means \pm standard error of the mean for others. Statistical significance was considered if $p < 0.05$ by two-tailed Student's t-test.

2 Supplementary Figures and Tables

Supplementary Figure 1. Representative pictures of the different vessel segments and transition points in ApoE^{-/-} and ApoE^{-/-}Fbn1^{C1039G+/-} mice. Pictures show the common carotid artery (CCA), the extracranial and intracranial internal carotid artery (ICA), vertebral artery (VA) and basilar artery (BA). In the ApoE^{-/-} mouse there was no plaque at the cranial site of the IC-Ptgpal bifurcation, the site of the vessel that is heading towards brain. The pictures of the ApoE^{-/-}Fbn1^{C1039G+/-} mouse are taken from the mouse with the most extensive atherosclerosis. The atherosclerotic plaque extends into the ICA running through the skull base, but stops just before the vessel enters the cranium. This mouse also has atherosclerosis in the extracranial vertebral artery, but not in the intracranial vertebral artery, basilar artery or any other arteries of the Circle of Willis like the posterior communicating artery (PCOM).



Supplementary Figure 2. Changes in vessel wall morphology in C57Bl/6 mice from the common carotid artery (CCA) to the intracranial part of the internal carotid artery (ICA) (n=6).



Supplementary Table 1: Primary antibodies, secondary steps and chromogens used for ApoE^{-/-} mouse tissue

<i>Primary Antibody</i>	<i>Catalogue number</i>	<i>Vendor</i>		<i>Pre-treatment</i>	<i>Dilution</i>	<i>Secondary antibody</i>
CD31	Dia310	Dianova	Hamburg, Germany	TE9.0	1:50	Alexa568 conjugated goat-a-mouse IgG1
Caveolin	610059	BD bioscience	Franklin Lakes, NJ, USA	TE9.0	1:200	Alexa633 conjugated goat-a-rabbit
Claudine-5	Ab53765	Abcam	Cambridge, The United Kingdom	TE9.0	1:200	Alexa633 conjugated goat-a-rabbit
eNOS	PA5-16887	Thermo	Fremont, CA, USA	TE9.0	1:50	Alexa633 conjugated goat-a-rabbit
HO-1	NBP-77460	Novus Biologicals	Farmingdale, NY, USA	TE9.0	1:50	Alexa633 conjugated goat-a-rabbit
ICAM-1	bs-0608R	Bioss Inc.	Beijing, China	TE9.0	1:50	Alexa633 conjugated goat-a-rabbit
SMA (1A4)	M0851	Dako	Glostrup, Denmark	TE9.0	1:200	Alexa633 goat-a-Mouse IgG2b
SM-MHC	Ab124679	Abcam	Cambridge, The United Kingdom	TE9.0	1:200	Alexa633 conjugated goat-a-rabbit
VCAM	bs-0920R	Bioss Inc.	Dallas, TX, USA	TE9.0	1:50	Alexa633 conjugated goat-a-rabbit
ZO1	617300	Life technologies	Carlsbad, CA, USA	TE9.0	1:50	Alexa633 conjugated goat-a-rabbit

Supplementary Table 2: Primary antibodies, secondary steps and chromogens used for C57Bl/6 mouse tissue

<i>Primary Antibody</i>	<i>Catalogue number</i>	<i>Vendor</i>		<i>Pre-treatment</i>	<i>Dilution</i>	<i>Secondary antibody</i>	<i>Chromogen</i>
Caveolin	610059	BD bioscience	Franklin Lakes, NJ, USA	Citr6.0	1:2000	Brightvision AP conjugated anti Rabbit	PermaBlue plus/AP
Claudine-5	Ab53765	Abcam	Cambridge, The United Kingdom	TE9.0	1:2000	Brightvision AP conjugated anti Rabbit	PermaBlue plus/AP
eNOS	PA5-16887	Thermo	Fremont, CA, USA	TE9.0	1:50	Brightvision AP conjugated anti Rabbit	PermaBlue plus/AP
Glut-1	Rb-9052	Thermo Fisher Scientific	Fremont, CA, USA	TE9.0	1:2000	Brightvision AP conjugated anti Rabbit	PermaBlue plus/AP
HO-1	Adi-spa-895	Enzo Lifesciences	Farmingdale, NY, USA	TE9.0	1:200	Brightvision AP conjugated anti Rabbit	PermaBlue plus/AP
ICAM-1	50440-R020	Sino Biological	Beijing, China	TE9.0	1:1000	Brightvision AP conjugated anti Rabbit	PermaBlue plus/AP
NQO1	Nb200-209	Novus Biologicals	Littleton, CO, USA	Citr6.0	1:500	Mouse on Mouse polymer bundle	Bright DAB
Nrf2	Ab31163	Abcam	Cambridge, The United Kingdom	TE9.0	1:100	Brightvision AP conjugated anti Rabbit	PermaBlue plus/AP
SMA (1A4)	M0851	Dako	Glostrup, Denmark	TE9.0	1:200	Gt-a-Ms-IgG2a/AP	PermaBlue plus/AP
SM-MHC	Ab124679	Abcam	Cambridge, The United Kingdom	TE9.0	1:2000	Brightvision AP conjugated anti Rabbit	PermaBlue plus/AP
VCAM	Sc-1504	Santa Cruz	Dallas, TX, USA	TE9.0	1:2000	Rabbit anti-Goat unlabeled 1:2000, Brightvision AP conjugated anti Rabbit	PermaBlue plus/AP
VE-Cadherin	Ls-132138	Life Span Biosciences	Seattle, WA, USA	Citr6.0	1:100	Brightvision AP conjugated anti Rabbit	PermaBlue plus/AP
ZO1	61-7300	Invitrogen	Carlsbad, CA, USA	Pepsin	1:200	Brightvision AP conjugated anti Rabbit	PermaBlue plus/AP

AP: Alkaline Phosphatase; Citr: citrate; DAB: 3,3'-Diaminobenzidine; eNOS: Endothelial nitric oxide synthase; Glut-1: Glucose transporter 1; HO-1: Heme oxygenase-1; ICAM-1: Intercellular Adhesion Molecule 1; NQO1: NAD(P)H dehydrogenase, quinone 1; Nrf2: Nuclear factor (erythroid-derived-2)-like; SMA: Smooth muscle actin; SM-MHC: Smooth muscle myosin heavy chain; TE: Tris-EDTA; VCAM: Vascular cell adhesion protein; VE-cadherin: vascular endothelial cadherin; ZO-1: zona occludens-1.

Supplementary Table 3: Patient characteristics

<i>Patient</i>	<i>Sex</i>	<i>Age</i>	<i>Cause of death</i>
1	M	87	Unknown
2	M	60	Neurological causes
3	F	64	Unknown
4	M	59	Neurological causes
5	M	58	Unknown
6	M	78	Unknown
7	F	72	Cardiovascular causes
8	F	87	Cardiovascular causes
9	F	65	Neurological causes
10	F	62	Neurological causes
11	F	92	Unknown
12	M	50	Neurological causes
13	F	66	Neurological causes
14	M	32	Unknown
15	M	68	Neurological causes
16	M	69	Infectious causes

Supplementary Table 4: Primary antibodies, secondary steps and chromogens used for human FFPE samples

<i>Primary Antibody</i>	<i>Catalogue number</i>	<i>Vendor</i>		<i>Pre-treatment</i>	<i>Dilution</i>	<i>Secondary antibody</i>
CD31 (JC70A)	M0823	Dako	Glostrup, Denmark	TE9.0	1:100	Alexa568 conjugated goat-a-mouse IgG1
HO-1	Adi-spa-895-D	Enzo Lifesciences	Farmingdale, NY	TE9.0	1:100	Alexa633 conjugated goat-a-rabbit
eNOS	PA5-16887	Thermo Fisher	Fremont, CA, USA	TE9.0	1:200	Alexa633 conjugated goat-a-rabbit
NRF2	383727	R&D systems	Minneapolis, MN, USA	TE9.0	1:50	Alexa633 conjugated goat-a-Mouse IgG2b

eNOS: Endothelial nitric oxide synthase; HO-1: Heme oxygenase-1; NRF2: Nuclear factor (erythroid-derived-2)-like ; TE: Tris-EDTA.

Supplementary table 5: All results from the stainings performed in the different experimental groups.

	Atherosclerosis models	ApoE ^{-/-}	C57Bl/6	Human samples
HE	√	√	√	-
EvG, elastin layers	-	√	√	-
HO-1	-	↗	↗	↗
eNOS	-	↗	↗	↗
NRF2	-	-	-	=
NQO1	-	-	↗	-
SMA	-	↗	↗	-
SM-MHC/SMA	-	√↗	=	-
Claudin-5	-	↗	↗	-
ZO-1	-	↗	=	-
VE-cadherin	-	-	=	-
ICAM1	-	=	√	-
VCAM1	-	↗	√↗	-
Caveolin	-	√↗	√↗	-
Glut-1	-	-	↗	-